

1 **The role of the winter residual circulation in the summer mesopause regions in**  
2 **WACCM**

3 Maartje Sanne Kuilman<sup>1</sup>, Bodil Karlsson<sup>1</sup>

4 <sup>1</sup>Department of Meteorology, Stockholm University, 10691 Stockholm, Sweden.

5 *Correspondence to:* Maartje Sanne Kuilman (maartje.kuilman@misu.su.se)

6

7 **Abstract**

8

9 High winter planetary wave activity warms the summer polar mesopause via a link  
10 between the two hemispheres. Complex wave – mean flow interactions take place on  
11 a global scale, involving sharpening and weakening of the summer zonal flow.  
12 Changes in the wind shear occasionally generate flow instabilities. Additionally, an  
13 altering zonal wind modifies the breaking of vertically propagating gravity waves. A  
14 crucial component for changes in the summer zonal flow is the equatorial  
15 temperature, as it modifies latitudinal gradients. Since several mechanisms drive  
16 variability in the summer zonal flow, it can be hard to distinguish which one that is the  
17 dominant. In the mechanism coined interhemispheric coupling, the mesospheric  
18 zonal flow is suggested to be a key player for how the summer polar mesosphere  
19 responds to planetary wave activity in the winter hemisphere. We here use the  
20 Whole Atmosphere Community Climate Model (WACCM) to investigate the role of  
21 the summer stratosphere in shaping the conditions of the summer polar. Using  
22 composite analyses, we show that in the absence of an anomalous summer  
23 mesospheric temperature gradient between the equator and the polar region, weak  
24 planetary wave forcing in the winter would lead to a warming of the summer  
25 mesosphere region instead of a cooling, and vice versa. This is opposing the  
26 temperature signal of the interhemispheric coupling that takes place in the  
27 mesosphere, in which a cold and calm winter stratosphere goes together with a cold  
28 summer mesopause. We hereby strengthen the evidence that the variability in the  
29 summer mesopause region is mainly driven by changes in the summer mesosphere  
30 rather than in the summer stratosphere.

31

32 **1 Introduction**

33

34 The circulation in the mesosphere is driven by atmospheric gravity waves (GWs).  
35 These waves originate from the lower atmosphere and as they propagate upwards,  
36 they are filtered by the zonal wind in the stratosphere (e.g., Fritts and Alexander,  
37 2003). Because of the decreasing density with altitude and as a result of energy

38 conservation, the waves grow in amplitude. At certain altitudes, the waves –  
39 depending on their phase speeds relative to the background wind - become unstable  
40 and break. At the level of breaking, the waves deposit their momentum into the  
41 background flow, creating a drag on the zonal winds in the mesosphere, which  
42 establishes the pole-to-pole circulation (e.g. Lindzen, 1981; Holton, 1982,1983;  
43 Garcia and Solomon, 1985). This circulation drives the temperatures far away from  
44 the state of radiative balance, by adiabatically heating the winter mesopause and  
45 adiabatically cooling the summertime mesopause (Andrews et al., 1987; Haurwitz,  
46 1961; Garcia and Solomon, 1985; Fritts and Alexander, 2003). The adiabatic cooling  
47 in the summer leads to temperatures sometimes lower than 130 K in the summer  
48 polar mesopause (Lübken et al.,1990). These low temperatures allow for the  
49 formation of thin ice clouds, the so-called noctilucent clouds (NLCs).

50  
51 Previous studies have shown that the summer polar mesosphere is influenced by the  
52 winter stratosphere via a chain of wave-mean flow interactions (e.g. Becker and  
53 Schmitz, 2003; Becker et al., 2004; Karlsson et al., 2009). This phenomenon, termed  
54 interhemispheric coupling (IHC), manifests itself as an anomaly of the zonal mean  
55 temperatures. Its pattern consists of a quadrupole structure in the winter hemisphere  
56 with a warming (cooling) of the polar stratosphere and an associated cooling  
57 (warming) in the equatorial stratosphere. In the mesosphere, these anomalies are  
58 reversed: there is a cooling (warming) in the polar mesosphere, and an associated  
59 warming (cooling) in the equatorial region. The mesospheric warming (cooling) in the  
60 tropical region extends to the summer mesopause (see e.g. Körnich and Becker,  
61 2010).

62  
63 These anomalies are responses to different wave forcing in the winter hemisphere. In  
64 order to explain how these anomalies come about we here briefly summarize the  
65 interhemispheric coupling mechanism for the case when the winter stratosphere is  
66 dynamically active, i.e. for a stratospheric meridional flow that is anomalously strong.  
67 The mechanism works in reverse when the meridional circulation in the stratosphere  
68 is anomalously weak A stronger planetary wave (PW) forcing in the winter  
69 stratosphere yields a stronger stratospheric Brewer-Dobson circulation (BDC). This  
70 anomalously strong flow yields an anomalously cold stratospheric tropical region and  
71 a warm stratospheric winter pole, due to the downward control principle (Karlsson et  
72 al., 2009).

73

74 Due to the eastward zonal flow in the winter stratosphere, GWs carrying westward

75 momentum propagate relatively freely up into the mesosphere where they break.  
76 Therefore, in the winter mesosphere, the net drag from GW momentum deposition is  
77 westward. When vertically propagating planetary waves break – also carrying  
78 westward momentum – in the stratosphere, the momentum deposited onto the mean  
79 flow decelerates the stratospheric westerly winter flow. To put it short, a weaker  
80 zonal stratospheric winter flow allows for the upward propagation of more GWs with  
81 an eastward phase speed, which, as they break reduces the westward wave drag  
82 (see Becker and Schmitz, 2003, for a more rigorous description).  
83  
84 This filtering effect of the zonal background flow on the GW propagation results in a  
85 reduction in strength of the winter-side mesospheric residual circulation when the  
86 BDC is stronger. This weakened meridional flow causes the mesospheric polar  
87 winter region to be anomalously cold and the tropical mesosphere to be anomalously  
88 warm (Becker and Schmitz, 2003, Becker et al., 2004 and Körnich and Becker, 2009).  
89  
90 The critical step for IHC is the crossing of the temperature signal over the equator.  
91 The essential region is here the equatorial mesosphere. Central in the hypothesis of  
92 IHC is that the increase (or decrease) of the temperature in the tropical mesosphere  
93 modifies the temperature gradient between high and low latitudes in the summer  
94 mesosphere, which influences the zonal wind in the summer mesosphere, due to  
95 thermal wind balance (see e.g. Karlsson et al., 2009 and Karlsson and Becker, 2016).  
96  
97 The zonal wind change in the summer mesosphere modifies the breaking level of the  
98 summer side GWs. In the case of a warming of the equatorial mesosphere - when  
99 the BDC is strong - the zonal wind is modified in such a way that the intrinsic wave  
100 speeds are reduced (e.g. Becker and Schmitz, 2003; Körnich and Becker, 2009).  
101 Consequently, the GWs break at a lower altitude and over a broader altitude range  
102 (see Becker and Schmitz, 2003), thereby shifting down the GW drag per unit mass.  
103 Hence, the strength of the meridional flow is reduced, and the adiabatic cooling of  
104 the summer polar mesopause region decreases, resulting in a positive anomalous  
105 temperature response (Karlsson et al., 2009; Körnich and Becker, 2009; Karlsson  
106 and Becker, 2016). In the case of an equatorial mesospheric cooling, the response is  
107 the opposite: the relative difference between the zonal flow and the phase speeds of  
108 the gravity waves increase to that they break at slightly higher altitudes, with an  
109 anomalous cooling of the summer polar mesopause as a result.  
110  
111 The IHC pattern was first found using mechanistic models (Becker and Schmitz,

112 2003) underpinned by observations of mesospheric conditions (Becker et al., 2004;  
113 Becker and Fritts, 2006). The pattern was then found in observational data (e.g.  
114 Karlsson et al., 2007; Gumbel and Karlsson, 2011; Espy et al., 2011; de Wit et al.,  
115 2016), in the Whole Atmosphere Community Climate Model (WACCM: Sassi et al.  
116 2004, Tan et al., 2012), in the Canadian Middle Atmosphere Model (CMAM: Karlsson  
117 et al. 2009), and in the high altitude analysis from the Navy Operational Global  
118 Atmospheric Prediction System - Advanced Level Physics High Altitude (NOGAPS-  
119 ALPHA) forecast/assimilating system (Siskind et al., 2011).

120

121 As described above, the temperature in the equatorial mesosphere is modified by the  
122 strength of the residual circulation in the winter mesosphere. Karlsson and Becker  
123 (2016) showed that the equatorial mesosphere is substantially colder in July than it is  
124 in January, while the winter mesosphere is significantly warmer (see their Fig. 1).

125 They proposed that this cooling of the equatorial region - cause by the strong  
126 mesospheric winter flow - modifies the breaking levels of the summer GWs  
127 throughout the July season, leading to additional cooling of the summer polar  
128 mesopause region. If - as hypothesized by Karlsson and Becker (2016) - the  
129 fundamental effect of the IHC is a cooling of the summer polar mesopauses, it would  
130 mean that the mechanism plays a more important role affecting the temperatures in  
131 the summer mesopause in the NH compared to that in the SH, since the weaker  
132 planetary wave activity in the SH results in an increased gravity wave drag and a  
133 strengthening of mesospheric poleward flow in the winter mesosphere: The  
134 equatorial mesosphere is adiabatically cooled more efficiently than when the winter  
135 mesospheric circulation is weak. Karlsson and Becker (2016) further hypothesized  
136 that in the absence of the equator-to-pole flow in the SH winter, the summer  
137 mesopause in the NH would be considerably warmer. To test the hypothesis, they  
138 used the KMCM to compare control simulations to runs without GWs in the winter  
139 mesosphere. The predicted responses were confirmed, and the results were also  
140 backed up by correlation studies using the Canadian Middle Atmosphere Model  
141 (CMAM30).

142

143 The IHC mechanism - as described above - is not the only driver of variability in the  
144 summer polar mesopause region. Another common feature in the summer  
145 mesosphere is the quasi 2-day wave (Q2DW; see e.g. Pendlebury, 2012), which is  
146 generated by baroclinic instability linked to the shear of the easterly flow in the  
147 summer stratosphere (Wu et al., 1996). Since variability in the summer stratospheric  
148 zonal flow also is related to the IHC mechanism, the two phenomena should be

149 closely coupled, as suggested by Gu et al. (2016). An indication of their  
150 interconnection is given by the following studies: a) Karlsson et al. (2007) found a  
151 strong anticorrelation between the noctilucent cloud occurrence and high latitude  
152 winter stratospheric temperatures, and b) Siskind and McCormack (2014) showed  
153 that enhanced Q2DW activity corresponded well in time with noctilucent cloud  
154 disappearance. Both studies covered the same years. Siskind and McCormack  
155 (2014) sought revision of the theory behind the IHC since they could not find  
156 indications of the conventional temperature and wind patterns associated with the  
157 proposed IHC mechanism. In the light of these findings, we hypothesize that while  
158 the Q2DW is associated with an enhanced PW activity in the winter hemisphere as  
159 suggested by e.g. Salby and Challenghan (2001) and shown by Gu et al. (2016) - and  
160 could plausibly be one of the main drivers of warming events in the summer  
161 mesosphere, particularly the SH summer (see e.g. Gu et al., 2015) - it cannot  
162 completely replace the conventional IHC. The two main arguments are:

163

164 i) The Q2DW does not explain why calm conditions in the winter stratosphere  
165 generate anomalously cold conditions in the summer mesosphere (e.g.  
166 Karlsson et al., 2009; Karlsson and Becker, 2016).

167

168 ii) If it were only the Q2DW that generated warming events in the summer  
169 mesosphere, these events would be insensitive to the residual circulation in  
170 the mesosphere. Strong PW activity leading to acceleration of the summer  
171 stratospheric jet – via a sharpened summer stratospheric temperature  
172 gradient - would generate baroclinic instability independently of the  
173 circumstances in the winter mesosphere. Therefore, removing GWs in the  
174 winter would not influence the summer mesospheric response. We test this  
175 hypothesis in this study by compositing monthly mean winters of high and low  
176 PW activity and comparing the outcomes with and without winter GWs. These  
177 results are presented in Section 3.2.

178

179 Since IHC is controversial, we find it important to use as many tools as possible to  
180 test - and to underpin - our arguments. In this study, the well-established WACCM,  
181 described in section 2.1 below, is used to endorse the results obtained with the not  
182 as widely-used - yet high-performing - KMCM. WACCM is in some aspects a more  
183 comprehensive model than KMCM. For example, a major difference is that WACCM  
184 contains interactive chemistry in the middle atmosphere, while KMCM does not.  
185 WACCM also uses a different parameterization for non-orographic GWs than KMCM.

186 KMCM uses a simplified dynamical core and convection scheme as compared to  
187 WACCM. For details about the KMCM see e.g. Becker et al., 2015. The WACCM is  
188 described in section 2. In section 3, we present the results from removing the gravity  
189 waves in the winter hemisphere on the summer mesosphere region in WACCM.  
190 Comparisons to the Karlsson and Becker (2016) study are discussed in section 3.1.  
191 In section 3.2 we examine the role of the summer stratosphere in shaping the  
192 conditions of the polar mesosphere when the winter mesospheric flow is absent.  
193 Our conclusions are summarized in Section 4.

194

195 Since the IHC mechanism has a more robust signal in the SH winter – NH summer,  
196 we choose to focus particularly on this period, namely July. Nevertheless, results  
197 from January are also shown for comparisons and for further discussion.

198

## 199 **2 Method**

200

### 201 **2.1 Model**

202

203 The Whole Atmosphere Community Climate Model (WACCM) is a so-called “high-top”  
204 chemistry-climate model, which spans the range of altitude from the Earth’s surface  
205 to an altitude of about 140 km. WACCM has 66 vertical levels of a resolution of ~1.1  
206 km in the troposphere above the boundary layer, 1.1-1.4 km in the lower  
207 stratosphere, 1.75 km at the stratosphere and 3.5 km above 65 km. The horizontal  
208 resolution is 1.9° latitude by 2.5° longitude (Marsh et al., 2013).

209

210 The model is a component of the Community Earth System Model (CESM), which is  
211 a group of model components at the National Center for Atmospheric Research  
212 (NCAR). WACCM is a superset of the Community Atmospheric Model version 4  
213 (CAM4) and as such it includes all the physical parameterizations of CAM4 (Neale et  
214 al., 2013).

215

216 WACCM includes parameterized non-orographic gravity waves, which are generated  
217 by frontal systems and convection (Richter et al., 2010). The orographic GW  
218 parameterization is based on McFarlane (1987), while the nonorographic GW  
219 propagation parameterization is based on the formulation by Lindzen (1981).

220

221 In this study, the F\_2000\_WACCM (FW) compset of the model is used, i.e. the  
222 model assumes present day conditions. There is no forcing applied: the model runs a

223 perpetual year 2000. Our results are based on a control run and perturbation runs. In  
224 the control run, the winter side residual circulation is included. In the perturbation  
225 runs, the equator-to-pole flow is removed by turning off both the orographic and the  
226 non-orographic gravity waves. It should however be noted that even though the GWs  
227 are turned off, there are still some resolved waves, such as inertial gravity waves and  
228 planetary waves that drive a weak meridional circulation. The model is run for 30  
229 years.  
230

### 231 **3 Results and discussion**

#### 232 **3.1 The effect of the winter residual circulation on the summer mesopause**

233 To investigate the effect of the winter residual circulation on the summer mesopause,  
234 we compare the control run, which includes winter GWs, with the perturbation runs.  
235 In the perturbation runs, the residual flow is removed by turning off the parameterized  
236 GWs in the winter hemisphere. The resolved waves, such as tides, inertial gravity  
237 waves and planetary waves are still there and drive a weak poleward flow, as already  
238 described in section 2.1.

239 We start by investigating the case for the NH summer (July) with the GWs turned off  
240 for the SH, where it is winter. Figure 1 shows the difference in zonal-mean  
241 temperature, zonal wind and gravity wave drag for July as a function of latitude and  
242 altitude, between the control run and the perturbation run: the run without the GWs  
243 in the winter minus the run with the GWs in the SH.

244 Figure 1.

245 From Fig. 1a, it is clear that there is a considerable increase in temperature in the NH  
246 summer mesopause region in the case for which there is no equator-to-pole flow in  
247 the SH winter. This change in temperature in the summer polar mesosphere can be  
248 understood as a result of changes in the wave-mean flow interactions. Without the  
249 GWs in the SH winter, the winter stratosphere and lower mesosphere are colder.  
250 This is because GWs in the winter hemisphere drive downwelling, adiabatically  
251 heating these regions (e.g. Shepherd, 2000).

252 Turning off the gravity waves in winter hemisphere changes the meridional  
253 temperature gradient in the summer hemisphere, as the equatorial mesosphere will  
254 be warmer. Thereby - via thermal wind balance - the zonal mesospheric winds are

255 modulated. It is also clear that the zonal flow at high latitudes accelerates for the  
256 case where there is no meridional flow in the SH winter. These findings correspond  
257 with what is found in Karlsson and Becker (2016).

258 Fig. 1a shows a significant warming in the equatorial mesosphere as well as in the  
259 stratosphere in the case where there are no GWs in the winter hemisphere,  
260 indicating a weakening of the BDC. We suggest that the warming of the tropical  
261 stratosphere could be due to a redistribution of PW momentum drag in the winter  
262 stratosphere: without GWs in the mesosphere, breaking levels of the westward  
263 propagating planetary waves are shifted upwards. Hence, the PW drag will be  
264 distributed over a wider altitude range. Our results show that this is indeed the case  
265 for the positive meridional heat flux (not shown). Another contributor to a decrease in  
266 the BDC is the removal of the orographic GWs, which act as PWs on the zonal flow  
267 in the winter stratosphere (see e.g. Karlsson and Becker, 2016; their figure 7).

268 The anomalously eastward flow in the summer upper stratosphere/lower  
269 mesosphere leads to lower GW levels and weaker GW drag over 45°N-70°N above a  
270 pressure level of 0.02 hPa as can be seen in Fig. 1b and c. This causes the summer  
271 polar mesopause to be considerably warmer. The temperature increase in the  
272 summer polar mesopause region, which is now loosely defined to be between 61°N -  
273 90°N and 0.01 - 0.002 hPa, is approximately 16 K. In a solely radiation-driven  
274 atmosphere, the temperature in the summer polar mesosphere is about 210-220 K,  
275 which is much higher than the temperature both with and without the GWs in the SH.

276 When comparing our results with the results in Karlsson and Becker (2016, their  
277 figure 3), we observe there are some quantitative discrepancies in the structure of  
278 the responses. For example, Karlsson and Becker (2016) found that removing the  
279 winter GWs resulted in a warming of the upper mesosphere globally, although the  
280 response was strongest in the polar mesopause region. They attributed the warming  
281 over the upper equatorial and winter mesosphere to the effect that GWs have on  
282 tides: when GWs are absent, the tidal response is enhanced. The same behavior is  
283 not found in WACCM - in fact, the equatorial upper mesosphere is anomalously  
284 cooler when the GWs are removed. These differences could perhaps be explained  
285 by for example the different gravity wave parameterization of non-orographic GWs,  
286 the different dynamical cores between the models and the presence of interactive  
287 chemistry in the middle atmosphere in WACCM.

288 However, the upper mesospheric response is not affecting the mechanism we are

289 discussing in this study. We do not consider the upper mesosphere region in the rest  
290 of the paper. The qualitative response of the temperature and zonal wind change in  
291 the stratosphere and lower parts of mesosphere due to turning off the GWs in the SH  
292 corresponds well with the results from the KMCM as well as with the hypothesis.

293 It can also be seen that in accordance with the results from the KMCM model, the  
294 zonal wind and temperature in summer stratosphere region change only slightly in  
295 the perturbation runs as compared to the control runs. We deem that anomalous GW  
296 filtering effects from lower down in the summer stratosphere, which could affect the  
297 results, are unlikely to contribute substantially to the temperature change in the  
298 summer mesosphere. We come back to this question in the next section 3.2.

299 Removing the gravity waves in the winter hemisphere leads to changes in the  
300 Eliassen-Palm (EP) flux divergence and in the residual circulation velocities  $\bar{v}^*$  and  
301  $\bar{w}^*$ . Fig. 1d shows that the EP flux divergence is changed mostly in the winter  
302 hemisphere, as expected, because the removal of GWs. The EP flux divergence  
303 increases in the stratosphere and decreases at higher altitudes. This could, as  
304 mentioned previously, be a result of the change in the zonal wind, which modifies the  
305 propagation and breaking of PWs in the winter stratosphere.

306 Fig. 1e and f show the changes in the residual circulation velocities. Again it is the  
307 winter hemisphere, which is mostly affected. As expected, for the case without GWs  
308 in the winter hemisphere, there is less southward flow as seen in Fig. 1e. At the  
309 same time  $\bar{w}^*$  changes throughout the winter stratosphere and mesosphere, as seen  
310 in Fig. 1f. There is a significantly stronger upwelling in the summer polar mesopause  
311 region as well as in the tropical mesosphere for the case when the GWs are included  
312 as compared to when they are absent (manifested by the negative anomalous  
313 response).

314 As pointed out before, the effect on the summer polar mesopause of removing winter  
315 GWs will be smaller in January than in July since the SH winter residual circulation is  
316 stronger than the NH summer mesosphere in July. Figure 3 shows the difference in  
317 zonal-mean temperature, zonal wind and gravity wave drag for January as a function  
318 of latitude and altitude, between the control run and the perturbation run: the run  
319 without the GWs in the NH winter hemisphere minus the run with the GWs in the NH  
320 winter hemisphere (similar to Fig. 1).

321 Figure 2.

322 From Fig. 2a, it can be observed that, in WACCM, there is no statistically significant  
323 temperature change in the SH summer polar mesopause region in the case for which  
324 there is no equator-to-pole flow in the NH winter. Without the GWs in the winter  
325 hemisphere, the winter stratosphere and lower mesosphere are colder, as in the July  
326 case. There is a change in zonal wind at high southern latitudes, but there is no clear  
327 statistical significant increase. These findings correspond with what is hypothesized  
328 in the introduction: taking away the GWs in the NH winter will have a weaker effect  
329 on the SH summer mesopause than taking away the GWs in the SH winter on the  
330 NH summer mesopause. This is plausibly partly due to the variable nature of the  
331 winter stratosphere zonal flow in the NH, which oscillates between being weak and  
332 strong. As a result, the January equatorial mesosphere is modified continuously: it  
333 varies between being adiabatically cooled and heated by the winter mesospheric  
334 residual flow. In July, on the other hand, the equatorial region is continuously cooled  
335 by the strong mesospheric residual flow in the SH winter. Hence, as already  
336 proposed by Karlsson and Becker (2016) the interhemispheric coupling mechanism  
337 gives one plausible explanation to why the July summer mesosphere region is  
338 considerably colder than the one in January.

339 We again show the effect of removing the gravity waves in the winter hemisphere on  
340 the Eliassen-Palm (EP) flux divergence and on the residual circulation velocities  $\bar{v}^*$   
341 and  $\bar{w}^*$ . Fig. 3d shows the difference in EP flux divergence, the pattern in the  
342 mesospheric response is similar to the response in July. Also the general patterns of  
343 the changes in residual circulation velocities (see Fig. 3e and f) look similar but are in  
344 general a bit smaller than in the July case, which we expected. Note the change of  
345 sign in  $\bar{v}^*$ , this is because the mesospheric flow in January is northwards as opposed  
346 to the flow in July.

347 Comparison between the responses found using WACCM with those found with  
348 KMCM (Karlsson and Becker, 2016, their Fig. 3), shows that the temperature change  
349 is larger and extends all the way to the summer pole in KMCM, while this is not the  
350 case in WACCM. However, the change in temperature in this region is not statically  
351 significant in WACCM. The differences in temperature and zonal wind responses are  
352 larger in January than in July when comparing the results of WACCM with that of  
353 KMCM. Nevertheless, the qualitative structure of the temperature and zonal wind  
354 change due to turning off the winter GWs corresponds convincingly well.

355 IHC has hitherto primarily been seen as a mode of internal variability giving rise to a

356 warming of the summer mesopause region. These results presented here and in  
357 Karlsson and Becker (2016) show the more fundamental role of interhemispheric  
358 coupling; the mechanism has a net cooling effect on the summer mesosphere.

359

### 360 **3.2 The effect of the summer stratosphere region on the summer mesopause**

361 The summer stratospheric meridional temperature gradient is affected by the  
362 strength of Brewer-Dobson circulation. Hence, filtering effects taking place below the  
363 mesosphere could be an additional - or alternative - mechanism to the response  
364 observed in the summer mesopause. Moreover, the Q2DW is amplified as a result of  
365 baroclinic instability associated with a strengthening of the easterly jet in the summer  
366 stratosphere (e.g. Gu et al., 2016). If Q2DWs were the sole reason for summer polar  
367 mesospheric warming events at dynamically active winters, the response would still  
368 hold after removing winter GWs. In this section, we will discuss why the variability in  
369 the summer stratosphere is unlikely to be the main driver to year-to-year temperature  
370 responses in the summer polar mesosphere. We focus again mostly on the NH  
371 summer polar mesosphere region.

372

373 In Fig. 3, the results from compositing years of high (a) and years of low (b)  
374 temperature anomalies, indicating high and low PW activity, in the winter  
375 stratosphere in July (1-10 hPa, 60°S-40°S) are shown for cases when GWs are  
376 present (upper panels) and absent (lower panels) in the winter hemisphere.  
377 Thresholds for the temperature anomalies are set as lower than half a standard  
378 deviation under the mean for the low temperature anomalies, and higher than half a  
379 standard deviation above the mean for the high temperature anomalies. As can be  
380 seen in the temperature responses associated with PW activity, the NH summer  
381 polar mesosphere is responding with the same anomalous sign as the high latitude  
382 winter stratosphere when winter GWs are included (Fig 3 a and b). This is in  
383 agreement with the results presented in Karlsson et al. (2009) although the WACCM  
384 temperature response does not reach statistical significance at a 95% level all the  
385 way to the polar region. This could be due to time lags between the response in the  
386 summer mesopause and the dynamic activity in the winter: Karlsson et al. (2009)  
387 found a lag between the winter and the summer hemisphere of up to 15 days. In the  
388 monthly-mean approach that we use for this study, lags in time are not accounted for.  
389 Nevertheless, as seen in the figure, when winter GWs are absent (lower panels) the  
390 anomalous temperature responses in the summer polar mesosphere and in the  
391 winter polar stratosphere are opposing each other (Fig. 3 c and d).

392

393 In terms of summer GW filtering and breaking, this opposing change in temperature  
394 response (Fig. 3c and d) can be understood by considering the anomalous response  
395 in the zonal flow. In Fig 4a - c, we show the absolute vertical profiles of the summer  
396 zonal wind, the summer GW drag between 45°N-70°N and the summer temperatures  
397 between 60°N-70°N for high (dashed black) and low (red) PW activity in the winter  
398 stratosphere for July when winter GWs are included. Figure 4 d-f show the difference  
399 between the profiles: the case without GWs minus the control case. The anomalous  
400 responses, i.e. deviations about the 30-year mean, are show in Fig. 4 g-i. As can be  
401 seen in Fig 4 a, d and g, the westward stratospheric flow is slightly enhanced during  
402 high PW activity. An anomalous easterly flow will increase the intrinsic phase speed  
403 of the summer GWs carrying eastward momentum, which would result in an increase  
404 of the GWs breaking levels. However, at high PW activity, the mesospheric wind  
405 shear (from westward towards eastward) is stronger than at low PW activity, as  
406 illustrated in Fig. a, d and g., and results in a lowering of the GW breaking level in the  
407 mesosphere compared to calm winter stratospheric conditions (Fig. 4b, e and h). As  
408 the GWs break lower, the adiabatic cooling of the summer polar mesopause is  
409 reduced, as seen in Fig. 4 c, f and i. Additionally, it is worth pointing out that an  
410 intensification of the zonal wind shear would naturally lead to baroclinic instability and  
411 generation of Q2DWs.

412 Fig. 5 shows profiles that are analogous to the ones illustrated in Fig. 4, but for the  
413 cases when winter GWs are absent. Note the differences in the wind profiles shown  
414 in 4 and 5. As described above, when the anomalous temperature response in the  
415 equatorial mesosphere is absent, the summer GWs carrying eastward momentum  
416 break slightly higher at high PW activity in the winter, as illustrated in Fig. 5 b, f and h  
417 leading to an anomalously cooler mesosphere (Fig. 5 c, f and i). Analogously, from  
418 Fig. 5, it is clear for a weak BDC (i.e. low PW activity), and therefore anomalously  
419 low temperatures in the SH winter stratosphere, the zonal winds in the stratosphere  
420 are less strongly westward. This leads to a weaker GW drag and a warmer NH  
421 summer mesopause region.

422

423 Our results show that without GWs in the SH winter hemisphere, the NH summer  
424 stratospheric variability - caused by the winter-side PW activity - has the major  
425 influence on the temperatures in the NH summer polar mesopause region. In the  
426 absence of the winter GWs, a dynamically active winter stratosphere leads to a  
427 cooling of the summer polar mesosphere instead of the warming associated with the

428 conventional interhemispheric coupling mechanism. Moreover, our study indicates  
429 that if Q2DWs are solely generated by the strengthening of the easterly stratospheric  
430 summer jet, they are not likely to be the major contributor for warming the summer  
431 polar mesopause region during high PW events in the winter: if they were, a warming  
432 of this region in the absence of winter GWs would still occur. However, we suggest  
433 that also the Q2DWs are related to conventional IHC since the anomalous quadruple  
434 temperature response in the winter middle atmosphere at high PW wave activity (e.g.  
435 Fig. 3 a) sharpens the wind shear between the stratosphere and the mesosphere in  
436 the summer hemisphere.

437 Fig. 6 – 8 illustrate the same as Fig. 3 – 5, but for January conditions. Even though  
438 the statistical significance of the results is not as high as for July, the same chain of  
439 arguments apply.

440 We conclude that for both hemispheres, the effect of PW activity on the summer  
441 polar mesosphere temperatures would be the opposite, if changes in the summer  
442 stratosphere were acting alone. Hence, the IHC as described by e.g. Karlsson et al.  
443 (2009) still holds as the dominant mechanism governing the monthly mean  
444 temperatures variability in the summer polar mesosphere, at least for July.

#### 445 **4 Conclusive summary**

446 In this study, the interhemispheric coupling mechanism and the role of the summer  
447 stratosphere in shaping the conditions of the summer polar mesosphere have been  
448 investigated. For the purpose, we have utilized the widely used WACCM model to  
449 carry out sensitivity experiments in the same manner as Karlsson and Becker (2016):  
450 the mesospheric residual flow in the winter hemisphere was dramatically diminished  
451 by removing winter GWs. This setting allows for studying the effect of summer  
452 stratospheric variability alone, i.e. without considering any influences from the winter  
453 mesospheric flow.

454

455 In accordance with Karlsson and Becker (2016), we find that the summer polar  
456 mesopause region would be substantially warmer without the gravity wave-driven  
457 residual circulation in the winter. Additionally, as for the KMCM experiment, we find  
458 using WACCM that the interhemispheric coupling mechanism has a net cooling  
459 effect on the summer mesospheres differing in magnitude between the two  
460 hemispheres, although signal in WACCM doesn't reach statistical significance all the

461 way to the poles. The mechanism plays a more important role affecting the  
462 temperatures in the NH summer mesopause compared to the SH.

463

464 In the absence of winter GWs - hence without the winter mesospheric residual  
465 circulation - the variability in the summer polar mesosphere is determined by the  
466 temperature gradient in the summer stratosphere below. However, the response  
467 opposes that of the conventional interhemispheric coupling: it is found that in the  
468 absence of winter gravity waves, low planetary wave activity in the winter  
469 hemisphere leads to a warming of the summer polar mesosphere region for both the  
470 northern and the southern hemispheres. Our results again confirm the idea that the  
471 IHC mechanism - with the equatorial mesosphere playing a crucial role - has a  
472 significant influence on the temperatures in the summer mesopause regions.

473

474 The Q2DW, a common feature in the summer mesosphere, is associated with an  
475 enhancement of the easterly flow in the summer stratosphere. The influence by  
476 these waves on the summer polar mesosphere can be rather dramatic. Nevertheless,  
477 our study shows that in a statistical sense, these events are of less importance for  
478 the summer polar mesosphere, at least if generated by the stratospheric flow alone.  
479 This conclusion is drawn from noting that anomalous easterly flow in the stratosphere  
480 gives rise to a cooling of the summer polar mesosphere if the mesospheric winter  
481 residual flow is absent. From this finding we suggest that the generation of the  
482 Q2DW is facilitated not only by an increase of the easterly summer stratospheric jet,  
483 but also by the conventional IHC mechanism, which increases the zonal wind shear  
484 between the summer stratosphere and mesosphere.

485

486

487

488

489

490

491

492

493

494

495

496

497

498

499

500

501

502

503

504 **References**

505

506 Andrews, D.G., Holton, J.R., Leovy, C.B.: Middle atmosphere dynamics, Academic  
507 Press, United States of America, 1987.

508

509 Becker E. and Fritts, D.C.: Enhanced gravity-wave activity and interhemispheric  
510 coupling during the MaCWAVE/MIDAS northern summer program 2002, Ann.  
511 Geophys., 24, 1175-1188, doi:10.5194/angeo-24-1175-2006, 2006.

512

513 Becker, E. and Schmitz, G.: Climatological effects of orography and land-sea  
514 contrasts on the gravity wave-driven circulation of the mesosphere, J. Atmos. Sci., 60,  
515 103-118, doi:10.1175/1520-0469(2003)060<0103:CEOAL>2.0.CO;2, 2003.

516

517 Becker, E., Müllermann, A., Lübken, F.-J., Körnich, H., Hoffmann, P., Rapp, M.: High  
518 Rossby-wave activity in austral winter 2002: Modulation of the general circulation of  
519 the MLT during the MaCWAVE/MIDAS northern summer program, Geophys. Res.  
520 Lett., 31, L24S03, doi:10.1029/2004GL019615, 2004.

521

522 Becker, E., R. Knöpfel and F.-J. Lübken, Dynamically induced hemispheric  
523 differences in the seasonal cycle of the summer polar mesopause. J. Atmos. Solar-  
524 Terr. Phys., 129, 128-141, doi:10.1016/j.jastp.2015.04.014, 2015.

525

526 De Wit, R.J., Janches, D., Fritts, D.C., Hibbins, R.E.: QBO modulation of the  
527 mesopause gravity wave momentum flux over Tierra del Fuego, Geophys. Res. Lett.,  
528 43, 4094-4055, doi:10.1002/2016GL068599, 2016.

529

530 Espy, P.J., Ochoa Fernández, S., Forkman, P., Murtagh, D., Stegman, J.:  
531 The role of the QBO in the inter-hemispheric coupling of summer mesospheric  
532 temperatures, Atmos. Chem. Phys., 11, doi:10.5194/acp-11-495-2011, 495-502,  
533 2011.

534

535 Fritts, D. C. and Alexander, M.J.: Gravity wave dynamics and effects in the middle  
536 atmosphere, Rev. Geophys., 41, 1003, doi:10.1029/2001RG000106, 2003.

537

538 Garcia, R.R., Solomon, S.: The effect of breaking gravity waves on the dynamics and  
539 chemical composition of the mesosphere and lower thermosphere, J. Geophys. Res.,  
540 90, D2, 3850-3868, doi:10.5194/10.1029/JD090iD02p03850, 1985.

541

542 Gu, S.-Y., Liu, H.-L., Li, T., Dou, X., Wu, Q., Russell III, J.M., Evidence of nonlinear  
543 interactions between quasi 2day wave and quasi-stationary wave, *J. Geophys. Res.*,  
544 120, 1256-1263, doi:10.5194/10.1002/2014JA020919, 2015.

545

546 Gu, S.-Y., Liu, H.-L., Pedatella, N.M., Dou, X., Li, T., Chen, T., The quasi 2day wave  
547 activities during 2007 austral summer period as revealed by the Whole Atmosphere  
548 Community Climate Model, *Journ. Geophys. Res. Space Physics*, 121, doi:  
549 10.1002/2015JA022225, 2016.

550

551 Gumbel, J., Karlsson, B.: Intra- and inter-hemispheric coupling effects on the polar  
552 summer mesosphere, *Geophys. Res. Lett.*, 38, L14804, doi:10.1029/2011GL047968,  
553 2011.

554

555 Haurwitz, B.: Frictional effects and the meridional circulation in the mesosphere, *J.*  
556 *Geophys. Res.*, 66, 8, doi:10.1029/JZ066i008p02381, 1961.

557

558 Holton, J.R.: The role of gravity wave induced drag and diffusion in the momentum  
559 budget of the mesosphere, *J. Atmos. Sci.*, 39, 791-799, doi:10.1175/1520-  
560 0469(1982)039<0791:TROGWI>2.0.CO;2, 1982.

561

562 Holton, J.R.: The influence of gravity wave breaking on the general circulation of the  
563 middle atmosphere, *J. Atmos. Sci.*, 40, 2497-2507, doi:10.1175/1520-  
564 0469(1983)040<2497:TIOGWB>2.0.CO;2, 1983.

565

566 Karlsson, B., Körnich, H., Gumbel, J.: Evidence for interhemispheric stratosphere-  
567 mesosphere coupling derived from noctilucent cloud properties, *Geophys. Res. Lett.*,  
568 34, L16806, doi:10.1029/2007GL030282, 2007.

569

570 Karlsson, B., McLandress, C., Shepherd, T.G.: Inter-hemispheric mesospheric  
571 coupling in a comprehensive middle atmosphere model, *J. Atmos. Sol.-Terr. Phys.*,  
572 71, 3-4, 518-530, doi:10.1016/j.jastp.2008.08.006, 2009.

573

574 Karlsson, B., Becker, E.: How does interhemispheric coupling contribute to cool  
575 down the summer polar mesosphere?, 29, 8807-8821, doi:10.1175/JCLI-D-16-  
576 0231.1, *J. Climate*, 2016.

577

578 Körnich, H. and Becker, E.: A simple model for the interhemispheric coupling of the  
579 middle atmosphere circulation, *Adv. in Space Res.*, 45, 5, 661-668,  
580 doi:10.1016/j.asr.2009.11.001, 2010.  
581

582 Lindzen, R.S.: Turbulence stress owing to gravity wave and tidal breakdown, *J.*  
583 *Geophys. Res.*, 86, C10, 9707-9714, 10.1029/JC086iC10p09707, 1981.  
584

585 Lübken, F.-J., Von Zahn, U., Manson, A., Meek, C., Hoppe, U.-P., Schmidlin, F.J.,  
586 Stegman, J., Murtagh, D.P., Rüster, R., Schmitz, G., Widdel, H.-U., Espy, P.: Mean  
587 state densities, temperatures and winds during the MAC/SINE and MAC/EPSILON  
588 campaigns, *J. Atmos. Sol.-Terr. Phys.*, 52, 10-11, 955-970,  
589 [https://doi.org/10.1016/0021-9169\(90\)90027-K](https://doi.org/10.1016/0021-9169(90)90027-K), 1990.

590 McFarlane, N. A.: The effect of orographically excited wave drag on the general  
591 circulation of the lower stratosphere and troposphere, *J. Atmos. Sci.*, 44, 1775–1800,  
592 10.1175/1520-0469(1987)044<1775:TEOOEG>2.0.CO;2, 1987.

593 Marsh, D. R., Mills, M.J., Kinnison, D.E., Lamarque, J.F., Calvo, N., Polvani, L.M.:  
594 Climate change from 1850 to 2005 simulated in CESM1(WACCM), 73727391, *J.*  
595 *Climate*, 26, 19, doi:10.1175/JCLI-D-12-00558.1, 2013.

596 Neale, R., Richter, J., Park, S., Lauritzen, P., Vavrus, S., Rasch, P., Zhang, M.: The  
597 mean climate of the Community Atmosphere Model (CAM4) in forced SST and fully  
598 coupled experiments, *J. Climate*, 26, 5150–5168, doi:10.1175/JCLI-D-12-00236.1,  
599 2013.

600 Pendlebury, D. A simulation of the quasi-two-day wave and its effect on variability of  
601 summertime mesopause temperatures, *J. Atmos. Sol.-Terr. Phys.*, 80, 138-151,  
602 <https://doi.org/10.1016/j.jastp.2012.01.006>.  
603

604 Richter, J. H., Sassi, F., Garcia, R.R.: Toward a physically based gravity wave  
605 source parameterization in a general circulation model, *J. Atmos. Sci.*, 67, 136–156,  
606 DOI: 10.1175/2009JAS3112.1, 2010.

607 Salby, M.L., Callaghan, P.F., Seasonal Amplification of the 2-Day Wave:  
608 Relationship between Normal Mode and Instability, *J. Atmos. Sci.*, 58, 1858-1869.

609 Sassi, F., Kinnison, D., Boville, B.A., Garcia, R.R., Roble, R.: Effect of El Niño-

610 Southern Oscillation on the dynamical, thermal, chemical structure of the middle  
611 atmosphere, *J. Geophys. Res.*, 109, D17108, doi:10.1029/2003JD004434, 2004.  
612

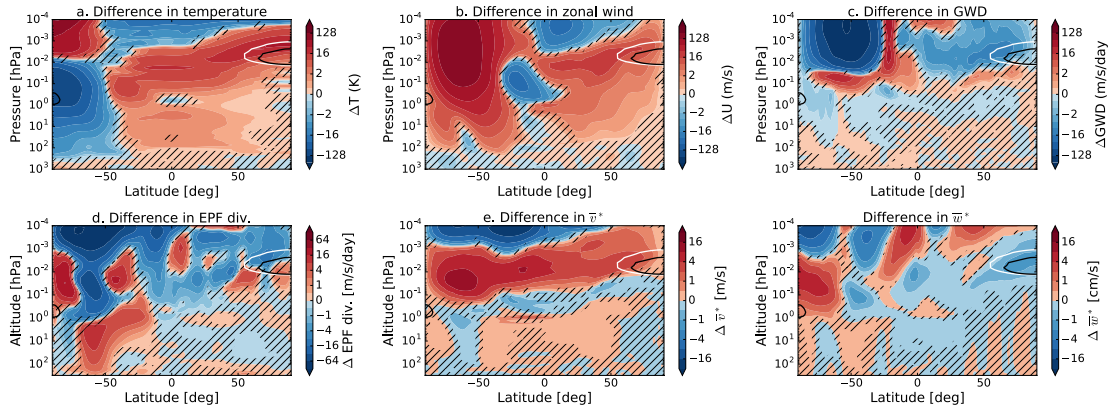
613 Shepherd, T.G., The middle atmosphere, *J. Atmos. Sol. Terr. Phys.*, 62, 17-18, 1587-  
614 1601, doi.org/10.1016/S1364-6826(00)00114-0, 2000.  
615

616 Siskind, D. E., Stevens, M.H., Hervig, M., Sassi, F., Hoppel, K., Englert, C.R.,  
617 Kochenas, A.J., Consequences of recent Southern Hemisphere winter variability on  
618 polar mesospheric clouds, *J. Atmos. Sol. Terr. Phys.*, 73, 2013–2021,  
619 10.1016/j.jastp.2011.06.014, 2011.  
620

621 Tan, B., Chu, X., Liu, H.-L., Yamashita, C., Russell III, J.M.: Zonal-mean global  
622 teleconnections from 15 to 110 km derived from SABER and WACCM, *J. Geophys.*  
623 *Res.*, 117, D10106, doi:10.1029/2011JD016750, 2012.  
624

625 Wu, D.L., Fishbein, E.F., Read, W.G., Waters, J.W., Excitation and evolution of the  
626 quasi-2-day-wave observed in UARS/MLS temperature measurements, *J. Atmos.*  
627 *Sci.*, 53(3), 728-738, [https://doi.org/10.1175/1520-](https://doi.org/10.1175/1520-0469(1996)053<0728:EAEOTQ>2.0.CO;2)  
628 [0469\(1996\)053<0728:EAEOTQ>2.0.CO;2](https://doi.org/10.1175/1520-0469(1996)053<0728:EAEOTQ>2.0.CO;2).  
629  
630  
631  
632  
633  
634  
635  
636  
637  
638  
639  
  
640  
  
641  
642  
643  
644  
645  
646

647



648

649

650

651

652

653

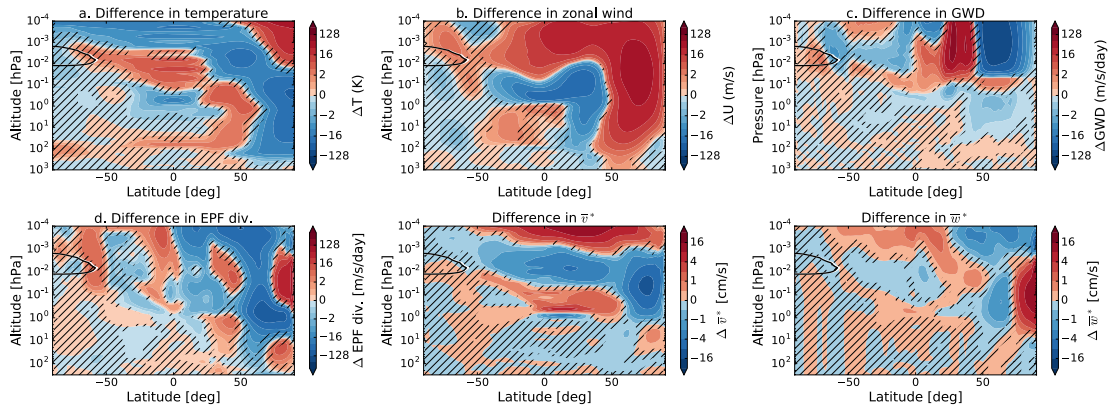
654

655

656

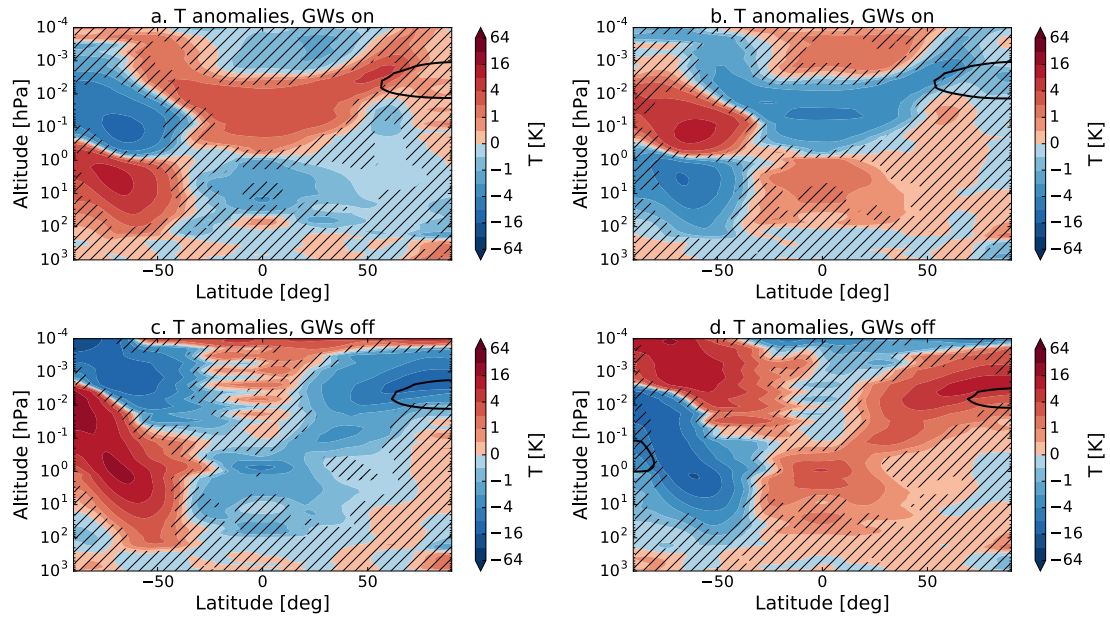
Fig. 1. The difference in zonal-mean temperature (a), zonal-mean zonal wind (b), gravity wave drag (c), EP flux divergence (d) and the transformed Eulerian-mean residual circulation velocity  $\bar{v}^*$  (e) and  $\bar{w}^*$  (f) for July: [run without winter GWs] minus [control run]. The white contour indicates the summer polar mesopause region where the temperatures are below 150 K for the control run. The black contour indicates the region where the temperature is below 150 K for the run without the GWs in winter. The shaded areas are regions where the data doesn't reach a confidence level of 95%.

657



658

Fig. 2. Same as Figure 1, but for January.



659

660

661

662

663

664

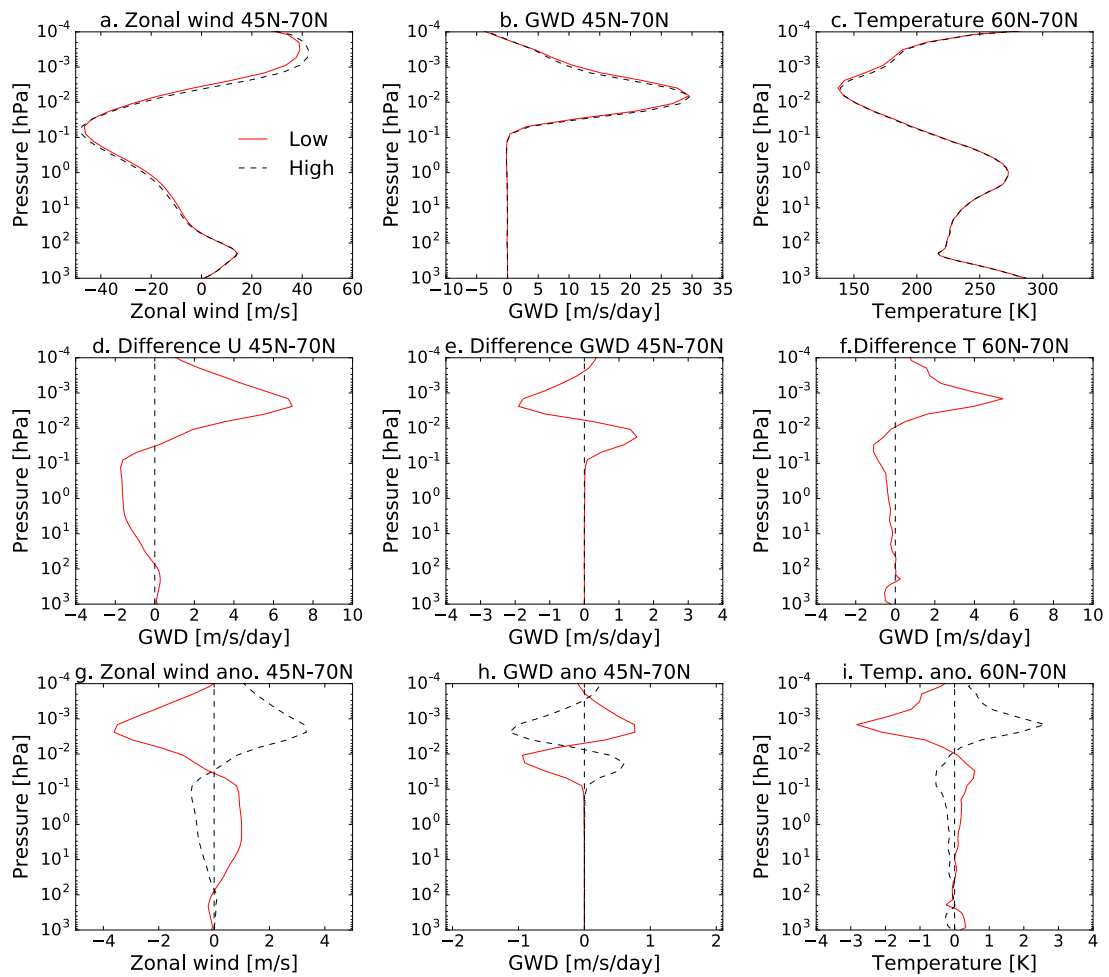
665

666

667

Fig. 3. The temperature anomalies for high (left) and low (right) planetary wave activity, as measured by the temperature in the winter stratosphere (1-10 hPa, 60°S-40°S) in July for the control run (first row) and run without GWs in the winter hemisphere (second row). There are 10 years of data with high temperature anomalies and 9 with low temperature anomalies in the winter stratosphere, this is the case for both the runs with and without the GWs in the winter hemisphere. The dotted areas are regions where the correlation has a p-value < 0.05. The black 150 K-contour indicates the polar mesopause region.

Control case



668

669 Fig. 4. The July zonal wind (left) and the GW drag (middle) between  $45^{\circ}$ -  $70^{\circ}$ N and  
 670 the temperature (right) between  $70^{\circ}$ - $90^{\circ}$ N for anomalously low and high temperatures  
 671 in the winter stratosphere ( $1$ - $10$  hPa,  $60^{\circ}$ S -  $40^{\circ}$ S) (first row) and the differences  
 672 between them (second row) and their anomalies (third row), for the case where there  
 673 are GWs in the winter hemisphere. The red continuous lines show the results for  
 674 anomalously low temperatures, the black dotted lines show the results for the  
 675 anomalously high temperatures.

676

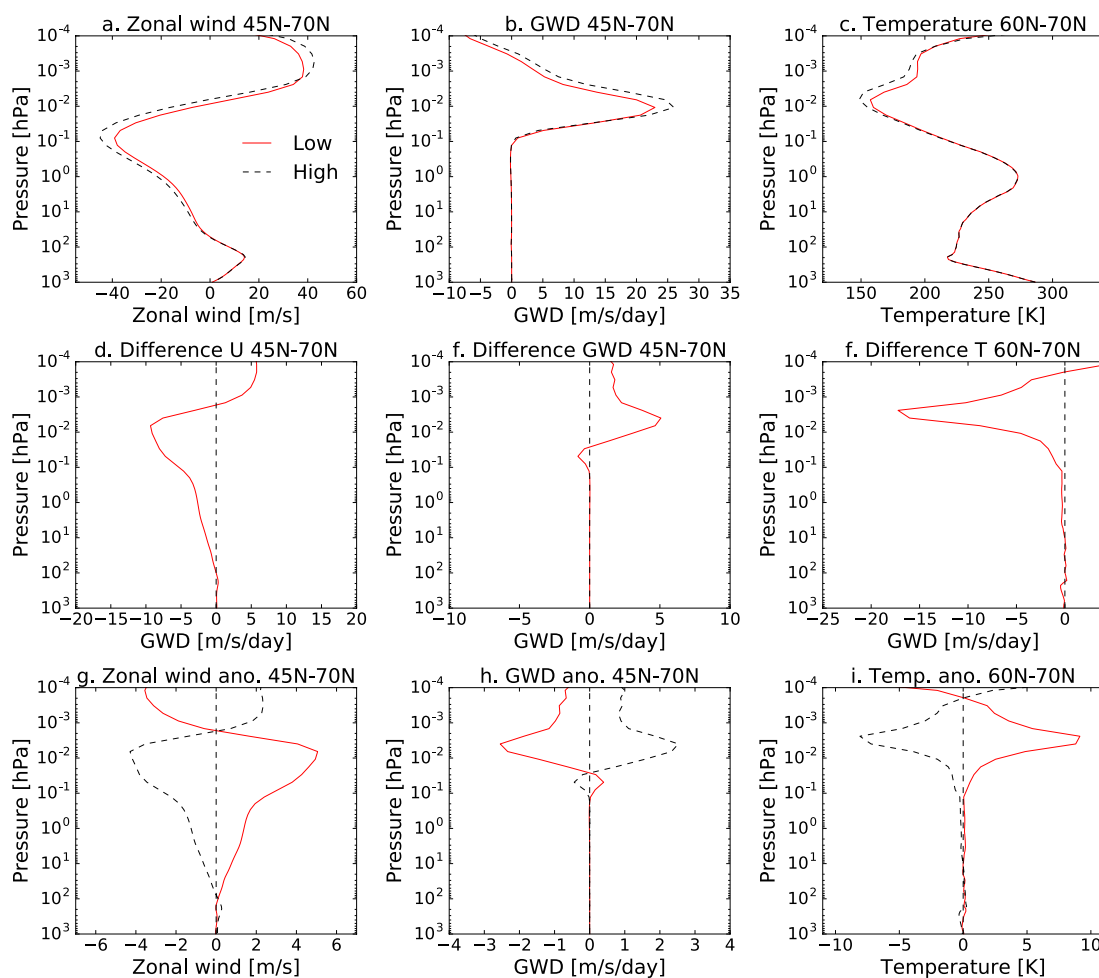
677

678

679

680

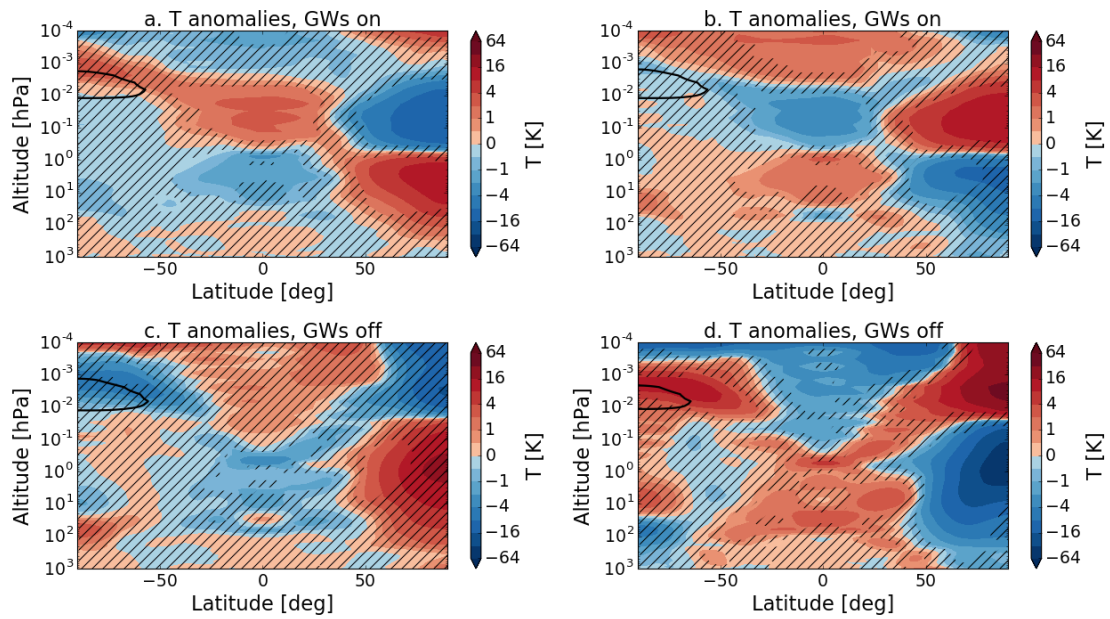
Run without GWs in the winter hemisphere



681

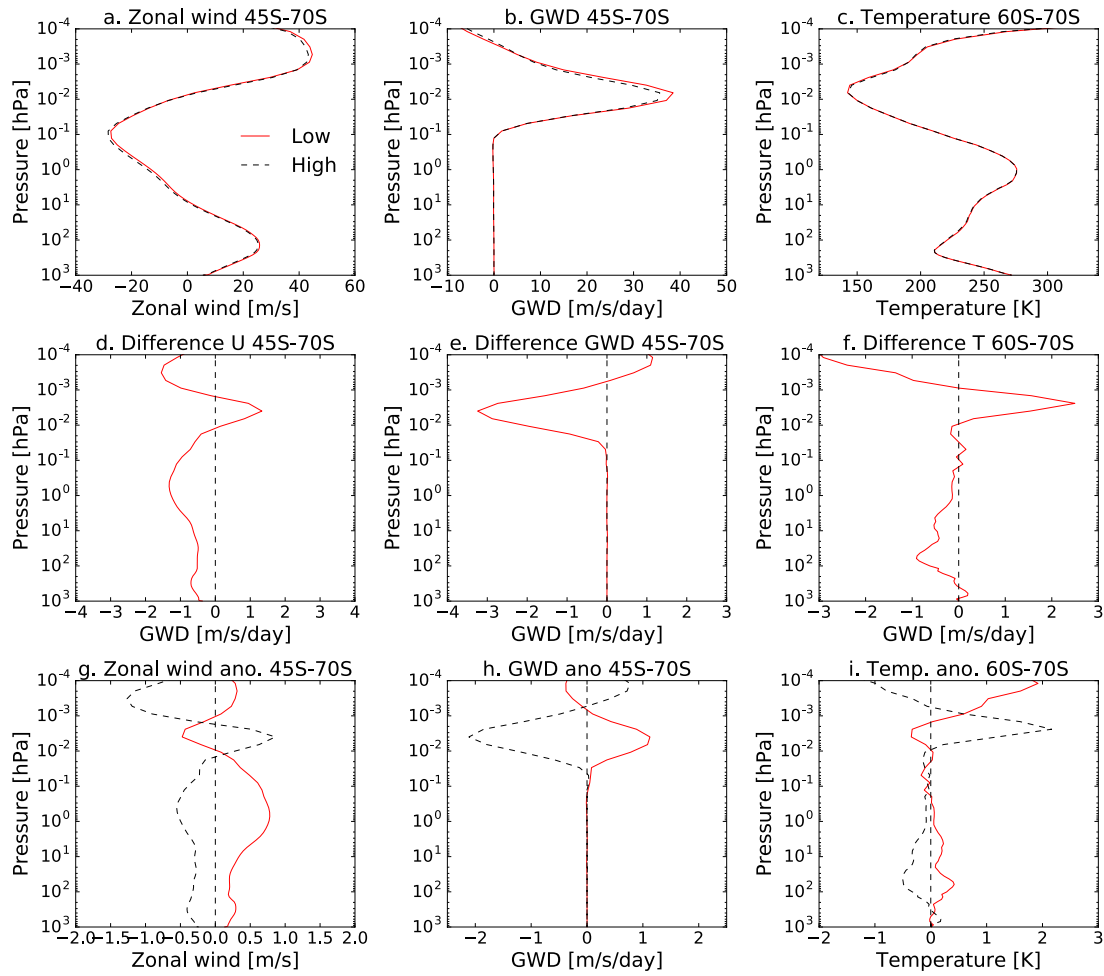
682 Fig. 5. The July zonal wind (left) and the GW drag (middle) between  $45^{\circ}$ -  $70^{\circ}$ N and  
 683 the temperature (right) between  $70^{\circ}$ - $90^{\circ}$ N for anomalously low and high temperatures  
 684 in the winter stratosphere ( $1$ - $10$  hPa,  $60^{\circ}$ S -  $40^{\circ}$ S) (first row) and the differences  
 685 between them (second row) and their anomalies (third row), for the case where there  
 686 are no GWs in the winter hemisphere. The red continuous lines show the results for  
 687 anomalously low temperatures, the black dotted lines show the results for the  
 688 anomalously high temperatures.

689



690  
 691 Fig. 6. The temperature anomalies for high (left) and low (right) planetary wave  
 692 activity, as measured by the temperature in the winter stratosphere (1-10 hPa, 50°N-  
 693 60°N) in January for the control run (first row) and run without GWs in the winter  
 694 hemisphere (second row). There are 10 years of data with high temperature  
 695 anomalies and 8 with low temperature anomalies in the winter stratosphere for the  
 696 control run. For the run without the GWs in the winter hemisphere, there are 7 years  
 697 with high temperature anomalies and 5 years with low temperature anomalies. The  
 698 dotted areas are regions where the correlation has a p-value < 0.05. The black  
 699 K-contour indicates the polar mesopause region.

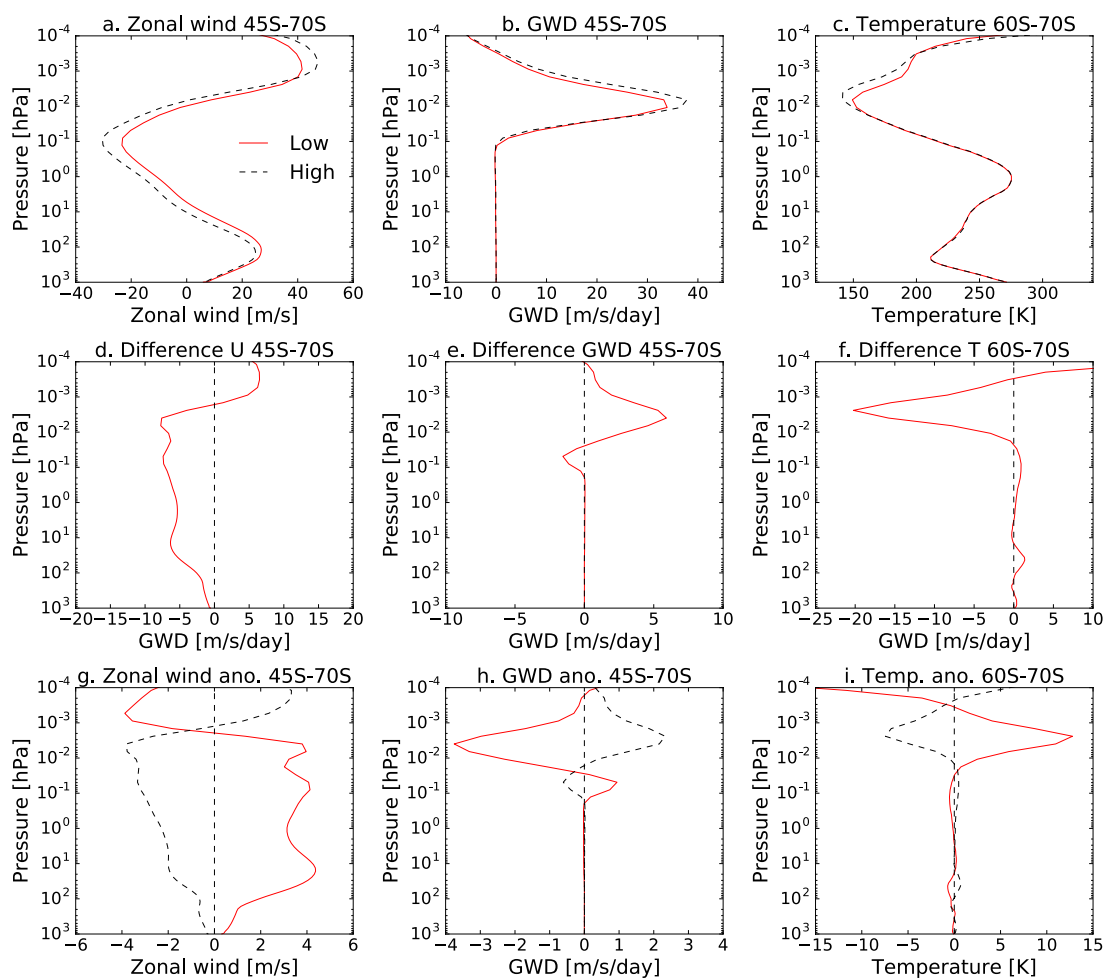
Control case



700

701 Fig. 7. The January zonal wind (left) and the GW drag (middle) between 45°- 70°S  
 702 and the temperature (right) between 60°S-70°S for anomalously low and high  
 703 temperatures in the winter stratosphere (1-10 hPa, 50°N - 60°N) (first row) and the  
 704 differences between them (second row) and their anomalies (third row), for the case  
 705 where there are GWs in the winter hemisphere. The red continuous lines show the  
 706 results for anomalously low temperatures, the red dotted lines show the results for  
 707 the anomalously high temperatures.

Run without GWs in the winter hemisphere



708

709 Fig. 8. The January zonal wind (left) and the GW drag (middle) between 45°- 70°S  
 710 and the temperature (right) between 60°S-70°S for anomalously low and high  
 711 temperatures in the winter stratosphere (1-10 hPa, 50°N - 60°N) (first row) and the  
 712 differences between them (second row) and their anomalies (third row), for the case  
 713 where there are no GWs in the winter hemisphere. The red continuous lines show  
 714 the results for anomalously low temperatures, the red dotted lines show the results  
 715 for the anomalously high temperatures.

716  
 717  
 718  
 719